X-622-71-519
PREPRINT

VERTICAL RESOLUTION OF TEMPERATURE PROFILES OBTAINED FROM REMOTE RADIATION MEASUREMENTS

BARNEY J. CONRATH

NOVEMBER 1971

X-622-71-519
Preprint

VERTICAL RESOLUTION OF TEMPERATURE PROFILES OBTAINED FROM REMOTE RADIATION MEASUREMENTS

by

Barney J. Conrath

November 1971

Laboratory for Planetary Atmospheres

Goddard Space Flight Center, Greenbelt, Maryland

VERTICAL RESOLUTION OF TEMPERATURE PROFILES OBTAINED FROM REMOTE RADIATION MEASUREMENTS

by

Barney J. Conrath

Laboratory for Planetary Atmospheres

Goddard Space Flight Center, Greenbelt, Maryland

ABSTRACT

The Backus-Gilbert theory, originally developed for analysis of inversion problems associated with the physics of the solid earth, is applied to the problem of the vertical sounding of the atmosphere by means of remote radiation measurements. An application is made to spectral intervals 2.8 cm^{-1} wide in the 667 cm^{-1} band of CO_2, and tradeoff curves are presented which quantitatively define the relationship between intrinsic vertical resolution and random error in temperature profile estimates. It is found that for a 1-2K random error with state-of-the-art instrumentation, the intrinsic vertical resolution ranges from $\sim$0.5 local scale height (l.s.h.) in the lower troposphere to > 2 l.s.h. in the upper stratosphere with $\sim$1 l.s.h. resolution in the vicinity of the tropopause. These values are somewhat smaller than the widths of the radiactive transfer kernels at similar levels. Increasing the number of spectral intervals from 7 to 16 is found to produce only a marginal improvement in vertical resolution.

VERTICAL RESOLUTION OF TEMPERATURE PROFILES OBTAINED FROM REMOTE RADIATION MEASUREMENTS

INTRODUCTION

One of the most significant contributions of the meteorological satellite program to date has been the development of techniques for the remote vertical sounding of the atmosphere. The Nimbus 3 and Nimbus 4 satellites carried instruments which provided measurements which could be used in the determination of vertical profiles of temperature, humidity, and ozone [Hanel and Conrath, 1969; 1970; Wark and Hilleary, 1969; Ellis, et al., 1970]. Extensive use has been made of these data in the development and application of atmospheric profile inversion techniques [see, for example, Smith, et al., 1970; Wark, 1970; Conrath, et al., 1970; Prabhakara, et al., 1970]. In addition to the obvious applications in terrestrial meteorology, remote vertical sounding techniques also provide a means for studying the atmospheres of other planets. Instrumentation has been developed for this purpose and is currently being flown on the Mariner 9 spacecraft for the 1971 Mars orbital mission [Hanel, et al., 1970].

One of the basic problems in the study of atmospheric profile inversion techniques concerns the vertical resolution and precision of the retrieved profiles. It has long been recognized that attempts to obtain better vertical resolution from a given set of data will result in an increase in sensitivity of the retrieved profiles to random noise. Therefore, in the analysis of a particular set of data there should be a tradeoff between the scale of features resolvable in an

estimated profile and its stability against noise. Up to the present time, no direct quantitative formulation has been given. Now, however, the recently developed theory of Backus and Gilbert [Backus and Gilbert, 1967; 1968; 1970; Backus, 1970a; 1970b; 1970c] can be employed in an analysis of the problem. Although the theory was developed for applications to inverse problems encountered in the physics of the solid earth, it is of quite general validity and can be easily adapted to the atmospheric profile inversion problem.

It is the purpose of the present paper to demonstrate the applicability of the work of Backus and Gilbert to atmospheric profile inversion and to make a specific application of the techniques to the problem of temperature profile estimation from measurements in the 667 cm^{-1} (15 μm) CO_2 absorption band in the terrestrial atmosphere.

A brief review of the formulation of Backus and Gilbert is first presented. Tradeoff curves are then calculated, using selected spectral intervals in the 667 cm^{-1} band. These curves quantitatively relate the vertical resolution of the retrieved profiles and their sensitivity to noise. The effect of varying the number of spectral intervals is examined. The averaging effect implicit in inversion calculations is studied in detail using the so-called "averaging kernels." Finally, conclusions are given concerning the intrinsic limitations of measurements obtained in the 667 cm^{-1} CO_2 band.

THE METHOD OF BACKUS AND GILBERT

The work of Backus and Gilbert has been confined primarily to the geophysical literature, so the techniques are generally unfamiliar to those working in atmospheric physics. Therefore, a brief review of the concepts of the method will be presented in this section. For a more thorough treatment of the theory, the reader is referred to the original literature, in particular, Backus and Gilbert [1967; 1968; 1970]. In addition, an excellent summary of the subject is given by Parker [1971].

Typically, in the remote sensing of atmospheric temperature profiles, measurements of radiances in a finite number of spectral intervals within an atmospheric absorption band are employed. For a non-scattering atmosphere in local thermodynamic equilibrium, a theoretical expression for the radiances can be written in the form

$$I_i = B_i(T_s)\tau_i(0) + \int_0^{x_t} B_i[T(x)] \frac{\partial \tau_i(x)}{\partial x} dx; \quad i = 1, 2, \cdots m. \tag{1}$$

In this expression, the independent variable x can be any monotonic function of the atmospheric pressure. In the following discussion, $x = -\ln P/P_s$ is employed where P_s is the surface pressure. Thus, x can be regarded as height expressed in terms of a local scale height (l.s.h.). In the i-th spectral interval, $B_i(T)$ is the Planck function for temperature T, and $\tau_i(x)$ is the atmospheric transmittance between level x and x_t, the effective top of the atmosphere. The term

$B_i(T_s)\,\tau_i(o)$ is the contribution from the planetary surface, here taken to be a blackbody at temperature T_s. The surface temperature and hence the boundary term, is usually specified from measurements in highly transparent spectral intervals.

The inversion problem then is to estimate the temperature profile T(x), given the atmospheric transmittances $\tau_i(x)$ and measurements of the radiances I_i ($i = 1, 2, \ldots m$). Let $T^\circ(x)$ be a reference profile in the neighborhood of the actual profile T(x). If the Planck function $B_i[T(x)]$ is expanded in a Taylor series at each level x about the reference profile $T^\circ(x)$, truncated after the linear term, and substituted into (1), there results

$$\Delta I_i = \int_0^{x_t} K_i(x)\,\Delta T(x)\,dx; \quad i = 1, 2, \cdots m. \tag{2}$$

The radiance difference is $\Delta I_i = I_i - I_i^\circ$ where I_i° is calculated from (1) using the reference profile, and $\Delta T(x) = T(x) - T^\circ(x)$. The quantities $K_i(x)$ ($i = 1, 2, \ldots m$) are given by

$$K_i(x) = \frac{dB_i[T^\circ(x)]}{dT}\,\frac{\partial \tau_i(x)}{\partial x} \tag{3}$$

and will be referred to as the radiative transfer kernels. For a finite number of measurements m, the set of linear integral equations (2) will possess either no solution or an infinite number of solutions for $\Delta T(x)$. The effects of this non-uniqueness must be considered in examining the vertical resolution obtainable with a given set of measurements.

Only estimates of $\Delta T(x)$ which are linear in the quantities obtained from measurements ΔI_i ($i = 1, 2, \ldots m$) will be considered. Such estimates can be written in the form

$$\hat{\Delta T}(x) = \sum_{i=1}^{m} a_i(x)\, \Delta I_i \tag{4}$$

where there will generally be a different set of coefficients $a_i(x)$ ($i = 1, 2, \ldots m$) for each value of x. If the expression for I_i given by (2) is substituted into (4), a relationship between the estimate $\hat{\Delta T}(x)$ and the actual profile $\Delta T(x)$ is obtained

$$\hat{\Delta T}(x) = \int_0^{x_t} A(x, x')\, \Delta T(x')\, dx' \tag{5}$$

where

$$A(x, x') = \sum_{i=1}^{m} a_i(x)\, K_i(x') \tag{6}$$

Thus, from (5), the estimate $\hat{\Delta T}(x)$ at a given level x can be regarded as a weighted average of the true profile with the weighting determined by the "averaging kernel" $A(x, x')$.

The vertical resolution of a particular linear estimate at the level x is determined by the behavior of $A(x, x')$. Ideally one would like for $A(x, x')$ to be a Dirac delta function. However, for a finite number of terms in (6) this is not possible, and $A(x, x')$ will have some finite spread about each level x. A useful measure of this spread has been given by Backus and Gilbert in the form

$$s(x) = 12 \int_0^{x_t} (x - x')^2 A^2 (x, x') \, dx' \tag{7}$$

The normalizing factor 12 is chosen such that when $A(x, x')$ is a rectangular function of width ℓ centered on x and satisfying

$$\int_0^{x_t} A(x, x') \, dx' = 1 \tag{8}$$

then $s(x) = \ell$. Other measures of the spread of $A(x, x')$ can be defined and several have been given by Backus and Gilbert. However, only (7) will be employed here.

Another parameter useful in characterizing the behavior of $A(x, x')$ is the "center" defined as

$$c(x) = \int_0^{x_t} x' A^2(x, x') \, dx' \Big/ \int_0^{x_t} A^2(x, x') \, dx' \tag{9}$$

and the "resolving length" of $A(x, x')$ can be defined as the spread about its center, i.e.,

$$w(x) = 12 \int_0^{x_t} [c(x) - x']^2 A^2 (x, x') \, dx'. \tag{10}$$

Thus, s(x) contains contributions both from the resolving length w(x) of $A(x, x')$ and from possible displacements of c(x) from x.

The maximum vertical resolution obtainable from a given set of radiance measurements using a linear estimation can be found by deriving the set of

coefficients $a_i(x)$ ($i = 1, 2, \ldots m$) which minimizes $s(x)$ subject to the constraint that the averaging kernel be unimodular, i.e., that is, satisfy (8). The requirement that $A(x, x')$ be unimodular insures that (5) will represent a well defined average.

Up to this point, consideration has not been given to the effects of measurement errors. In practice, instrument noise will result in an imprecise determination of ΔI_i. This noise contaminated value can be written

$$\tilde{\Delta I}_i = \Delta I_i + \epsilon_i \tag{11}$$

where ϵ_i is the unknown error in the measured value of I_i. The variance of the temperature error $\sigma_T^2(x)$ incurred at level x due to random measurement errors can be found from (4) to be

$$\sigma_T^2(x) = \mathbf{a}(x) \cdot \mathbb{E} \cdot \mathbf{a}(x)$$

where $\mathbf{a}(x)$ is the vector whose elements are the coefficients $a_i(x)$ ($i = 1, 2, \ldots m$), and $\mathbb{E}$ is the covariance tensor for the measurement errors.

Ideally one would like to be able to choose $\mathbf{a}(x)$ such that both the error variance $\sigma_T^2(x)$ and the spread $s(x)$ are minimized. This cannot be done, but it is possible to minimize a linear combination of $s(x)$ and $\sigma_T^2(x)$. Such a linear combination can be written

$$Q(x) = q s(x) + (1 - q)\, r\, \sigma_T^2(x). \tag{13}$$

The coefficient r insures that both terms have the same physical dimensions, but its numerical value is of no fundamental importance. By varying the parameter q between zero and unity, the emphasis can be shifted from minimization of the error to minimization of the spread. Thus, there is a tradeoff between vertical resolution and accuracy, and the best choice for q must be determined by the particular application.

In carrying out the minimization of Q(x), it is convenient to introduce the vector $\mathbb{u}$ whose components are given by

$$u_i = \int_0^{x_t} K_i(x)\, dx;\ i = 1,\ 2,\ \cdots m \tag{14}$$

and the tensor $\mathbb{S}(x)$ whose components are

$$S_{ij}(x) = 12 \int_0^{x_t} (x - x')^2\, K_i(x')\, K_j(x')\, dx';\ i,\ j = 1,\ 2,\ \cdots m. \tag{15}$$

If further, a tensor $\mathbb{W}(x;\ q)$ is defined by

$$\mathbb{W}(x;\ q) = q\, \mathbb{S}(x) + (1 - q)\, r\, \mathbb{E} \tag{16}$$

then the problem becomes one of minimizing

$$Q(x;\ q) = a \cdot \mathbb{W} \cdot a \tag{17}$$

subject to the constraint

$$\mathbf{a} \cdot \mathbf{u} = 1. \tag{18}$$

A straightforward minimization calculation gives

$$a(x;\ q) = \frac{W^{-1}(x;\ q) \cdot \mathbf{u}}{\mathbf{u} \cdot W^{-1}(x;\ q) \cdot \mathbf{u}} \tag{19}$$

Thus, for a particular value of q, the coefficients for a given level x can be calculated using (19). The resulting averaging kernel $A(x, x'; q)$, the spread $s(x; q)$, and the error $\sigma_T(x;q)$ can then be obtained from (6), (7), and (12). By varying q, the error σ_T can be obtained as a function of spread s. The resulting relationship is called the "tradeoff curve" and can be used to analyze the tradeoff between vertical resolution and errors in the estimated temperature due to random errors in the measurements. One such curve is obtained for each atmospheric level considered.

The Backus and Gilbert formulation provides a means of examining the intrinsic vertical resolution of temperature profiles obtained from infrared radiance measurements by means of linear inversion. In addition, the formulation provides inversion coefficients which can be employed in the actual reduction of data. However, only the analysis of vertical resolution will be considered further in the present paper.

APPLICATION TO THE 667 CM^{-1} BAND

The formulation reviewed in the preceeding section has been applied to an analysis of the vertical resolution of temperature profiles inferred from measurements in the 667 cm^{-1} (15μm) CO_2 band. The sixteen 2.8 cm^{-1} wide spectral intervals employed in the study are listed in Table 1. The kernels for a subset of seven spectral intervals denoted by asterisks in Table 1 are shown in Figure 1.

In order to characterize the behavior of the ith kernel, a mean atmospheric level $\bar{x}_i$ and a width d_i about the mean were defined, analogous to the center (9) and resolving length (10) of the averaging kernel, i.e.,

$$\bar{x}_i = \int_0^{x_t} x K_i^2(x)\,dx \Big/ \int_0^{x_t} K_i^2(x)\,dx \tag{20}$$

$$d_i = 12\, u_i^{-2} \int_0^{x_t} (x - \bar{x}_i)^2 K_i^2(x)\,dx. \tag{21}$$

The factor u_i^{-2} in (21), where u_i is given by (14), is to provide normalization of the kernel. The mean levels are given in Table 1 in terms of pressure, along with the width expressed in terms of local scale heights.

In calculating tradeoff curves, it was assumed that no correlation existed in the measurement noise of the various spectral intervals and that the noise variance was the same for all intervals. These assumptions are generally valid for measurements obtained in the portion of the spectrum being considered

here. In this case the error covariance tensor becomes

$$\mathbf{E} = \sigma_\epsilon^2 \, \mathbf{1} \tag{22}$$

where $\mathbf{1}$ is the unit tensor, and σ_ϵ^2 is the variance of the measurement noise. Relation (12) then reduces to the form

$$\frac{\sigma_T(x)}{\sigma_\epsilon} = [a(x) \cdot a(x)]^{1/2} \tag{23}$$

Thus, the tradeoff curves can be expressed as $\sigma_T(x)/\sigma_\epsilon$ vs. $s(x)$, and can be applied to measurements from an instrument with arbitrary noise level.

Tradeoff curves were calculated for many atmospheric levels. Examples are shown in Figure 2 to illustrate the behavior of the tradeoff curves in the troposphere, near the tropopause, and in the stratosphere. In each case two curves are shown, one for the full set of 16 spectral intervals listed in Table 1, and one for the 7-interval subset denoted in the table by asterisks. The results shown were obtained using a midlatitude temperature profile. Similar calculations were carried out with a tropical temperature profile, but the results were not substantially different from those shown in Figure 2.

The gross behavior of the tradeoff curves is the same for all levels. The random error decreases monotonically with increasing spread. The decrease is rapid at small values of the spread, followed by a rather abrupt leveling off with increasing spread. The end point of the curve corresponding to minimum spread and maximum random error corresponds to a choice of $q = 1$ in (13) while the

opposite end of the curve for which σ_T is a minimum and s is a maximum corresponds to q = 0. In the latter case, the inversion coefficients a are independent of atmospheric level, and the random error is the same for all levels. The steep portion of the tradeoff curve shifts in the direction of increasing spread as the atmospheric level increases, so for a given value of σ_T/σ_ϵ, the spread is greater for upper atmospheric levels than for lower levels.

Comparison of the tradeoff curves for 7 and 16 spectral intervals in Figure 2 indicates the degree of improvement which can be expected by increasing the number of spectral intervals. The minimum random error corresponding to the maximum spread is a factor of 1.45 higher for the 7-interval set than for the 16-interval set, reflecting the change in redundancy by a factor of approximately 2 in this case. In the steeper portion of the curves which is of greater practical interest, use of the 16-interval set results in only a small reduction in the spread for a given value of σ_T/σ_ϵ.

From the inversion coefficients $a(x)$ calculated for a given choice of q, the corresponding averaging kernel $A(x, x')$ can be obtained using (6). It is instructive to examine the behavior of $A(x, x')$ for typical cases. Figure 3 shows averaging kernels for the 7 spectral interval set at the 49 mb level, with each curve corresponding to a selected point on the tradeoff curve shown in Figure 2f. The value of s and σ_T/σ_ϵ for each curve is indicated in Figure 3. The averaging kernel in Figure 3a corresponds to minimum random error and maximum spread while at the opposite end of the tradeoff curve is the averaging kernel in

Figure 3f corresponding to minimum spread and maximum random error. The remaining curves in Figure 3 show the evolution of the averaging kernel in passing from one end point of the tradeoff curve to the other. Figure 4 shows averaging kernels for several tropospheric and stratospheric levels. In each case σ_T/σ_ϵ = 4 K/(erg/sec cm^2 ster cm^{-1}) except for the 49 mb level. In the case of the 49 mb level, the maximum value of σ_T/σ_ϵ reached by the 7-interval tradeoff curve is 1.6 K/(erg/sec cm^2 ster cm^{-1}) (see Figure 2h), and the corresponding averaging kernel is shown. Typical noise levels obtainable for measurements in this spectral region are 0.25 to 0.5 erg/cm^2 sec ster cm^{-1}, so a choice of σ_T/σ_ϵ = 4 K/(erg/sec cm^2 ster cm^{-1}) corresponds to a random error in the estimated temperatures of 1 to 2 K which is an acceptable level for most applications. Comparison of the averaging kernels of Figure 4 with the radiative transfer kernels of the original set of integral equations (Figure 1 and Table 1) shows that for comparable atmospheric levels the averaging kernels are narrower, although the 10 mb averaging kernel closely approaches the radiative transfer kernel for spectral interval 1 (667.5 cm^{-1}) in width.

Since the spread s(x) contains contributions both due to the width of the averaging kernel and the noncoincidence of its center with the level to which it pertains, it is instructive to examine the center and width (as measured by the resolving length) separately. The center, calculated using (9) is plotted as a function of atmospheric level in Figure 5, and the resolving length, calculated from (10), is given in Figure 6 for a value of σ_T/σ_ϵ = 4 K/(erg/sec cm^2 ster cm^{-1}).

The 16 spectral interval set was employed in this example. The center lies very close to the appropriate atmospheric level from the surface up to about 10 mb, but remains almost constant above that level. The abrupt increase in resolving length above 50 mb reflects the fact that most of the information on this region is coming from the 667.5 cm^{-1} interval for which the radiative transfer kernel is quite broad (see Table 1 and Figure 1).

The curves of Figures 5 and 6 indicate that little intrinsic information on the temperature profile above 10 mb is contained in measurements in this set of spectral intervals. The vertical resolution becomes very poor, and since the center of the averaging kernel does not move much above 10 mb, temperature estimates for the upper stratosphere will merely reflect the behavior of the temperature profile at lower levels.

Vertical resolution is best in the lower troposphere where the radiative transfer kernels are least broad. The vertical resolution in the vicinity of the tropopause (100 - 200 mb) is particularly interesting because of the relatively fine scale structure in the temperature profile which frequently exists there. From figure 6 it is found that the resolving length in this region is 0.8 - 1.0 l.s.h. which is considerably broader than the scale of the structure one would like to resolve. Some improvement in resolution can be gained by allowing the random error in the inferred temperatures to become larger. However, due to the steepness of the tradeoff curves, only a slight improvement in resolution can be obtained before the errors become intolerably large.

SUMMARY AND CONCLUSIONS

The theory of Backus and Gilbert, developed for applications to inverse problems of the physics of the solid earth, has been shown to be useful for the analysis of remote vertical atmospheric sounding systems. Tradeoff curves obtainable from the theory can be employed to define the limitations of measurements in a given set of spectral intervals. The curves can be used for the evaluation of the intrinsic information content of the measurements within the framework of linear inversion.

Analysis of 2.8 cm^{-1} wide spectral intervals in the 667 cm^{-1} CO_2 band indicates that for random temperature errors limited to 1-2 K with present state-of-the-art instrumentation, the intrinsic vertical resolution (measured in terms of the resolving length (10)) ranges from $\sim$0.5 l.s.h. in the lower troposphere to >2 l.s.h. in the upper stratosphere. The resolving length in the vicinity of the tropopause is $\sim$1 l.s.h. Comparison of the kernels of the original set of radiative transfer equations with the averaging kernels corresponding to 1-2 K random temperature errors indicates that linear inversion can provide somewhat better vertical resolution than the width of the radiative transfer kernels along would indicate. However, the resolution is still too coarse for the direct retrieval of certain fine scale features of interest, such as those required for an accurate determination of tropopause temperature and height.

Attempts at improving the vertical resolution by picking points on the tradeoff curves corresponding to smaller spread will generally be unsatisfactory.

Because of the steepness of the tradeoff curves in the region of interest, a small improvement in vertical resolution results in a large increase in random temperature error. Going to a large number of spectral intervals does not greatly improve the resolution. It was found that increasing the number of spectral intervals from 7 to 16 gave only marginal improvement in resolution at a given random error level. The only practical way to obtain resolutions significantly better than those indicated by the resolving lengths in Figure 6 with this set of spectral intervals is to supplement the intrinsic information content of the measurements with additional a priori information on the profile. This may be accomplished for example through a careful selection of the reference profile $T^{\circ}(x)$ or through a full statistical estimation approach such as that of Rodgers [1966] and Strand and Westwater [1968].

The analysis indicates that little information can be obtained on the temperature profile above the 10 mb level with the set of spectral intervals considered. Temperature estimates obtained for levels above 10 mb will in fact be primarily dependent on the behavior of the profile at lower levels. However, this situation can be improved through the use of measurements at higher spectral resolution which results in kernels which peak at higher atmospheric levels. Measurements of this type have been obtained successfully by Houghton and his colleagues, [Ellis, et al., 1970].

Only the diagnostic properties of the Backus-Gilbert theory have been explored here. The theory also provides a method of inversion, and this aspect is a subject of current study.

REFERENCES

Backus, G. E., 1970a: Inference from Inadequate and Inaccurate Data, I. Proc. Nat. Acad. Sci., 65, 1-7.

Backus, G. E., 1970b: Inference from Inadequate and Inaccurate Data, II. Proc. Nat. Acad. Sci., 65, 281-287.

Backus, G., 1970c: Inference from Inadequate and Inaccurate Data, III. Proc. Nat. Acad. Sci., 67, 282-289.

Backus, G. E., and J. F. Gilbert, 1967: Numerical Applications of a Formalism for Geophysical Inverse Problems. Geophys. J. R. Astr. Soc., 13, 247-276.

Backus, G. E., and J. F. Gilbert, 1968: The Resolving Power of Gross Earth Data. Geophys. J. R. Astr. Soc., 16, 169-205.

Backus, G. E., and J. F. Gilbert, 1970: Uniqueness in the Inversion of Inaccurate Gross Earth Data. Phil. Trans. R. Soc. London, A266, 123-192.

Conrath, B. J., R. A. Hanel, V. G, Kunde, and C. Prabhakara, 1970: The Infrared Interferometer Experiment on Nimbus 3. J. Geophys. Res. 75, 5831-5857.

Ellis, P. J., G. Peckham, S. D. Smith, J. T. Houghton, C. G. Morgan, C. D. Rodgers, and E. J. Williamson, 1970: First Results from the Selective Chopper Radiometer on Nimbus 4. Nature, 228, 139-142.

Hanel, R. A., and B. J. Conrath, 1969: Interferometer Experiment on Nimbus 3: Preliminary Results. Science, 165, 1258-1260.

Hanel, R. A., and B. J. Conrath, 1970: Thermal Emission Spectra of the Earth and Atmosphere from the Nimbus 4 Michelson Interferometer Experiment. Nature, 228, 143-145.

Hanel, R. A., B. J. Conrath, W. A. Hovis, V. Kunde, P. D. Lowman, C. Prabhakara, and B. Schlachman, 1970: Infrared Spectrometer Experiment for Mariner Mars 1971. Icarus, 12, 48-62.

Parker, R. L., 1970: The Inverse Problem of Electrical Conductivity in the Mantle. Geophys. J. R. Astr. Soc., 22, 121-138.

Prabhakara, C., B. J. Conrath, R. A., Hanel, and E. J. Williamson, 1970: Remote Sensing of Atmospheric Ozone Using the 9.6 Micron Band. J. Atmos. Sci., 27, 689-697.

Rodgers, C. D., 1966: Satellite Infrared Radiometer; A Discussion of Inversion Methods. Univ. of Oxford Clarendon Lab. Mem. 66.13, 25 pp.

Smith, W. L., H. M. Woolf, and W. J. Jacob, 1970: A Regression Method for Obtaining Real-Time Temperature and Geopotential Height Profiles from Satellite Spectrometer Measurements and its Application to Nimbus 3 "SIRS" Observations. Monthly Weather Review, 98, 582-603.

Strand, O. N., and E. R. Westwater, 1968: Minimum RMS Estimation of the Numerical Solution of a Fredholm Integral Equation of the First Kind. SIAM J. Numer. Anal., 5, 287-295.

Wark, D. Q., 1970: SIRS: An Experiment to Measure the Free Air Temperature from a Satellite. Applied Optics, 9, 1761-1766.

FIGURE CAPTIONS

Figure 1. Radiative transfer kernels for the 667 cm^{-1} CO_2 absorption band. The numbers labeling the curves refer to spectral intervals listed in Table 1.

Figure 2. Tradeoff curves for the 667 cm^{-1} CO_2 absorption band. σ_T is the standard deviation of the temperature error due to a random measurement error with standard deviation σ_ϵ. The atmospheric pressure level to which each curve pertains is indicated. The solid curves are for a set of 16 spectral intervals while the broken curves are for a 7-interval set.

Figure 3. Averaging kernels for the 49 mb level corresponding to selected points along the tradeoff curve shown in Figure 2f. The values of $\sigma_T / \sigma_\epsilon$ and the spread s are indicated in each case.

Figure 4. Averaging kernels for selected atmospheric levels. The level to which each kernel pertains is indicated by both a label and a broken line.

Figure 5. The averaging kernel center plotted as a function of atmospheric pressure level (solid curve). If the center of the kernel exactly coincided with the level to which the kernel pertained, the broken line would result.

Figure 6. The resolving length plotted as a function of atmospheric level. The resolving length provides a measure of vertical resolution.

Table 1

Characteristics of 667 cm^{-1} CO_2 Band Radiative Transfer Kernels

Interval	Central Frequency (cm^{-1})	Mean Level (mb)	Width (Local Scale Heights)
1*	667.5	13.1	2.42
2*	677.5	61.2	1.55
3	682.5	66.6	1.60
4	687.5	74.0	1.52
5	692.5	76.2	1.53
6*	697.5	92.7	1.78
7*	702.5	153.3	1.95
8*	707.5	286.9	1.65
9	712.5	403.3	1.47
10*	727.5	564.7	1.19
11	732.5	547.0	1.30
12	737.5	575.2	1.20
13	742.5	609.1	1.12
14*	747.5	692.9	0.92
15	752.5	740.8	0.74
16	757.5	798.6	0.59

*Spectral intervals employed in 7-interval set.

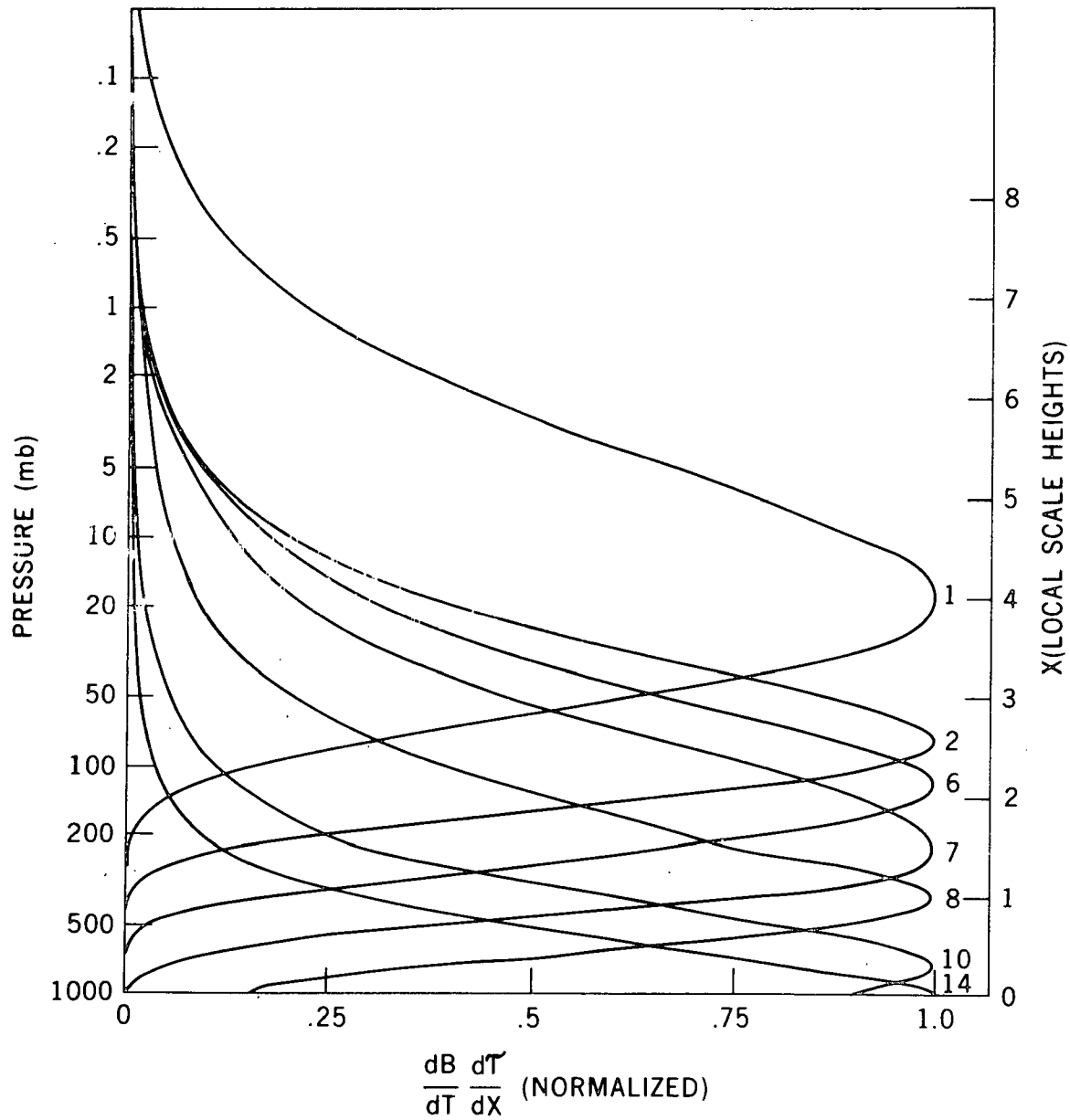

Figure 1. Radiative transfer kernels for the 667 cm^{-1} CO_2 absorption band. The numbers labeling the curves refer to spectral intervals listed in Table 1.

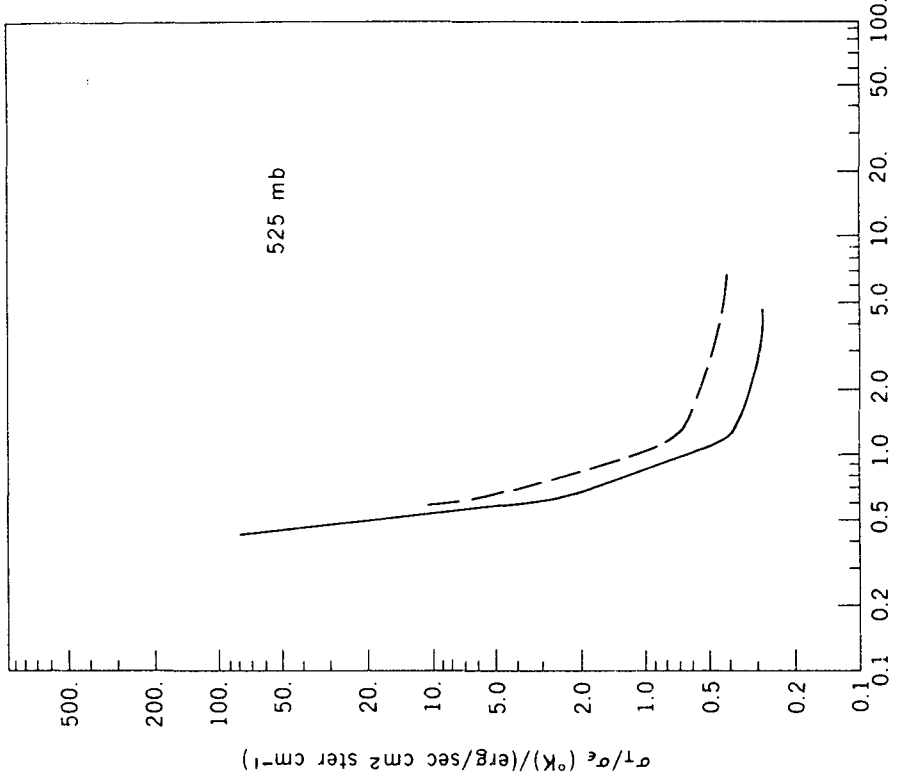

Figure 2(b).

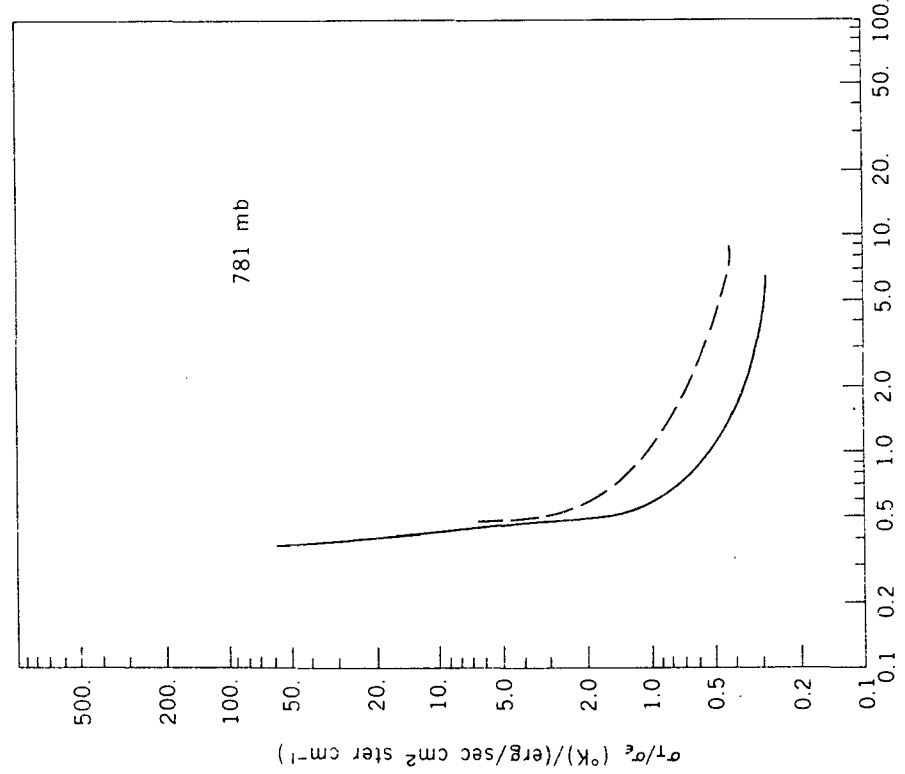

Figure 2(a).

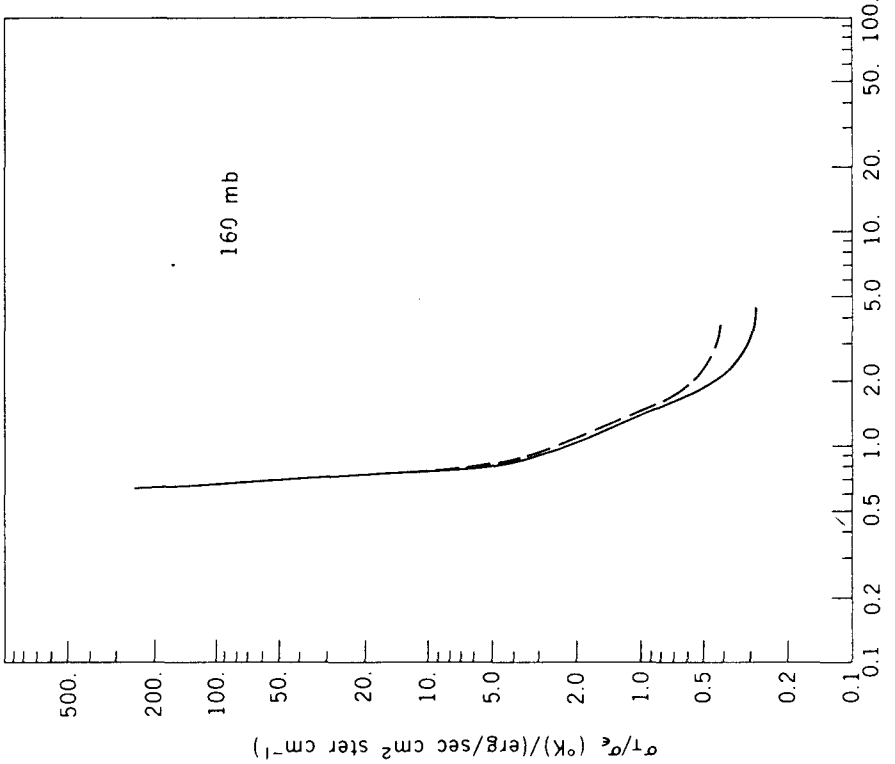

Figure 2(d).

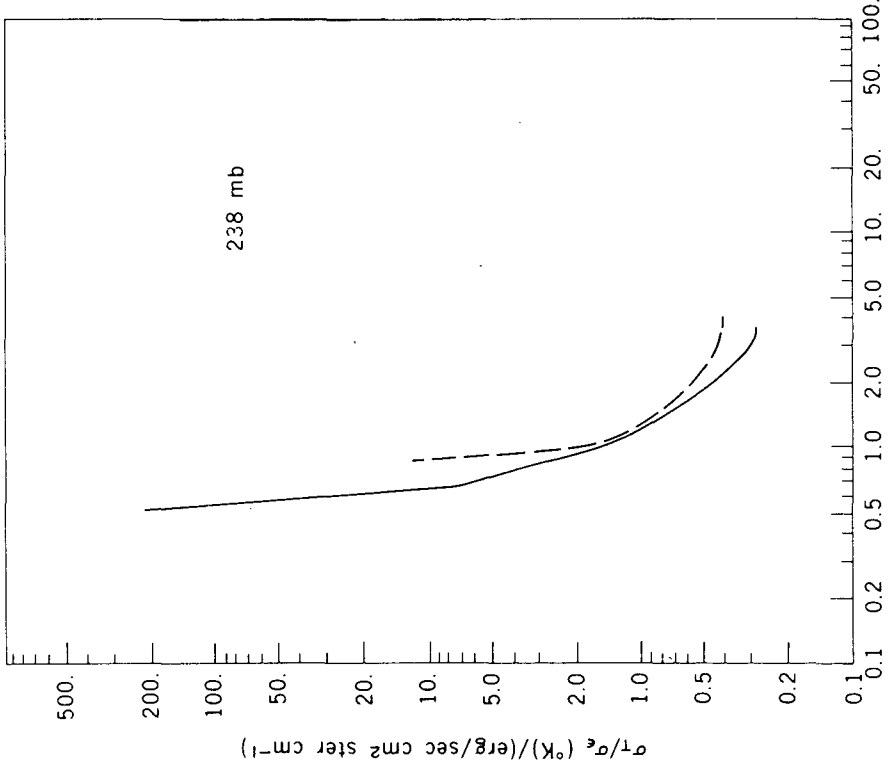

Figure 2(c).

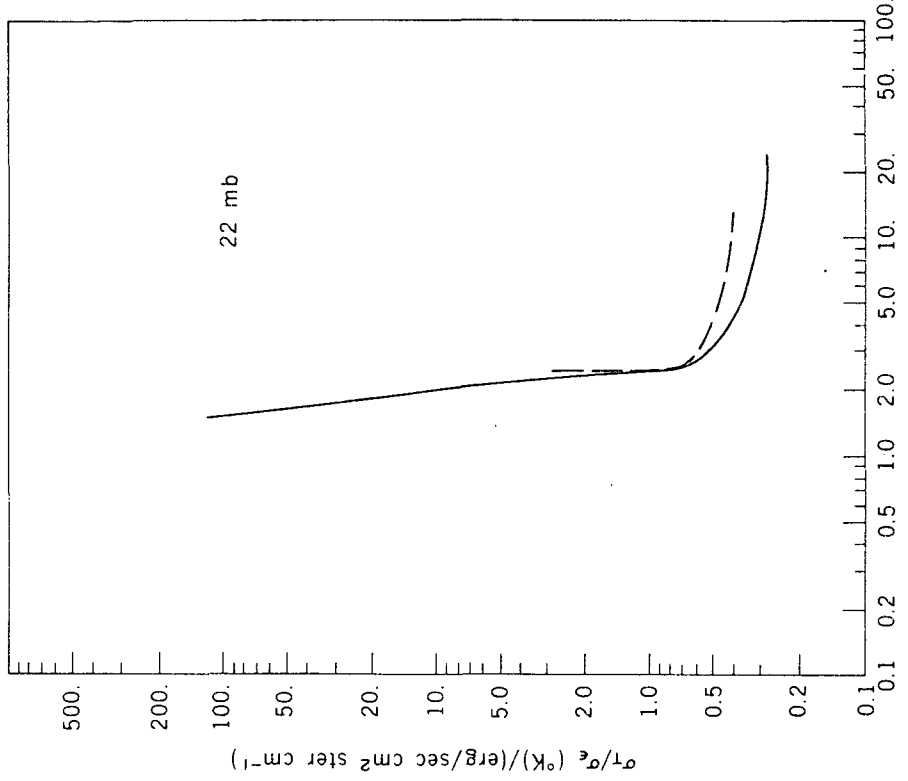

Figure 2(f).

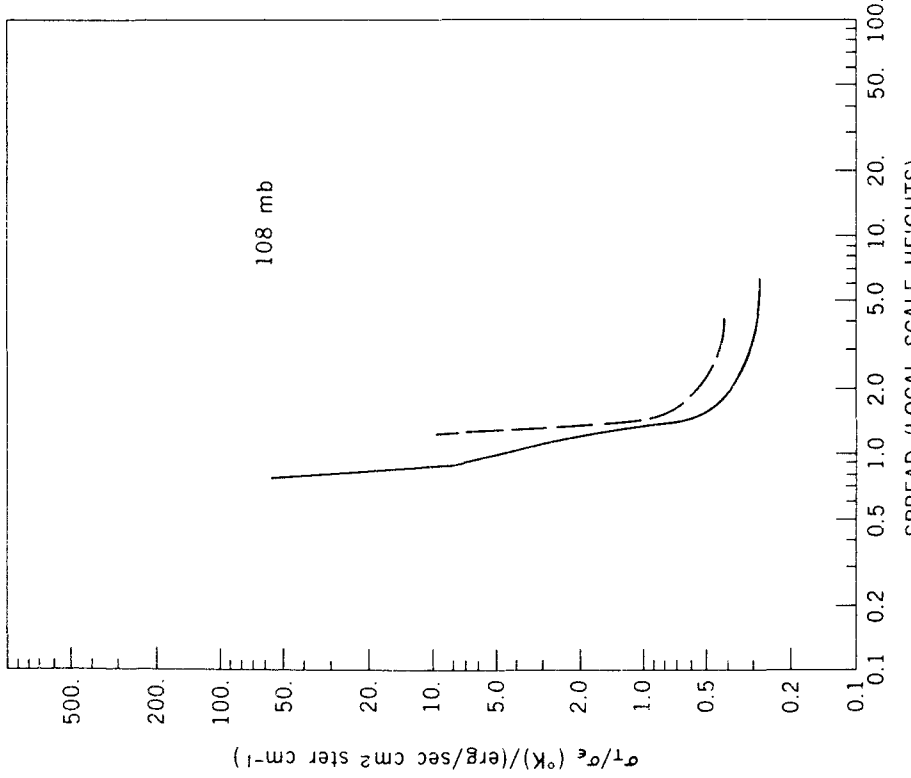

Figure 2(e).

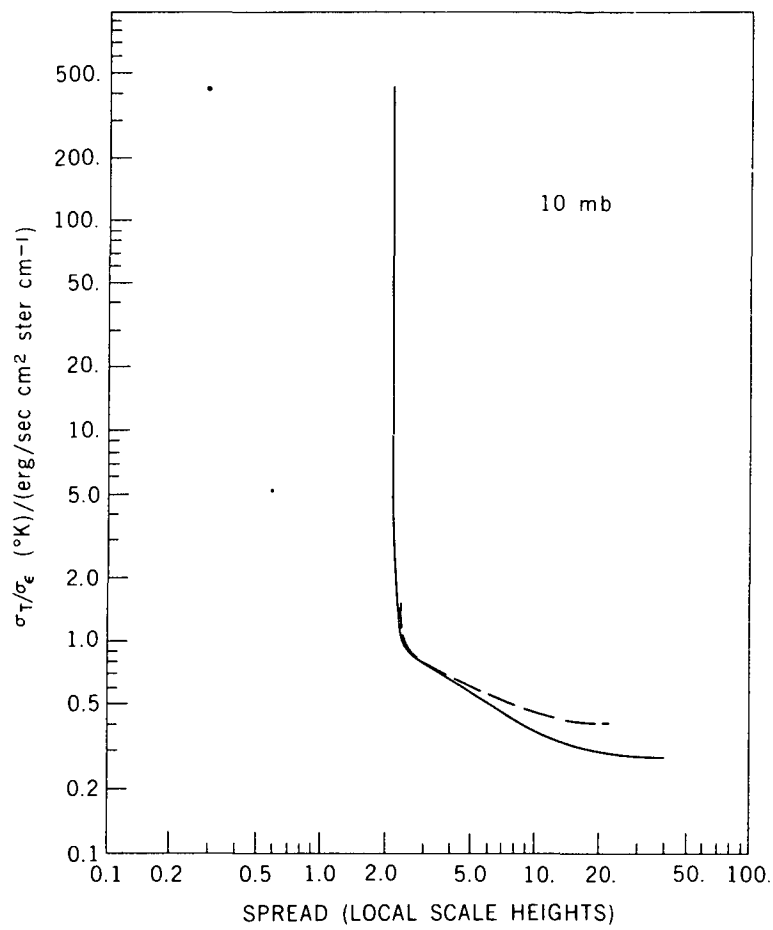

Figure 2(g).

Figure 2. Tradeoff curves for the 667 cm^{-1} CO_2 absorption band. σ_T is the standard deviation of the temperature error due to a random measurement error with standard deviation σ_ϵ. The atmospheric pressure level to which each curve pertains is indicated. The solid curves are for a set of 16 spectral intervals while the broken curves are for a 7-interval set.

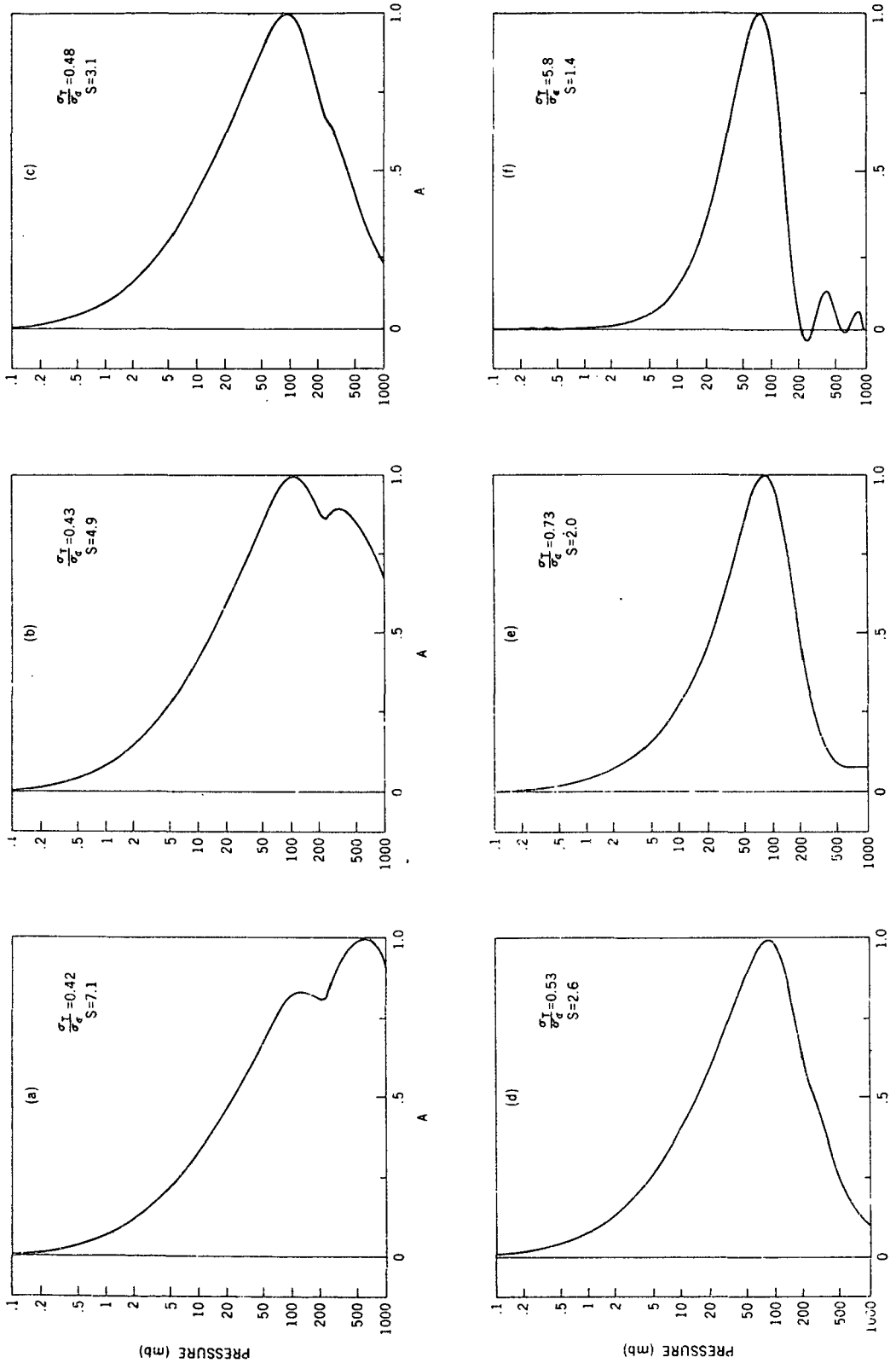

Figure 3. Averaging kernels for the 49 mb level corresponding to selected points along the tradeoff curve shown in Figure 2f. The values of σ_T/σ_ϵ and the spread s are indicated in each case.

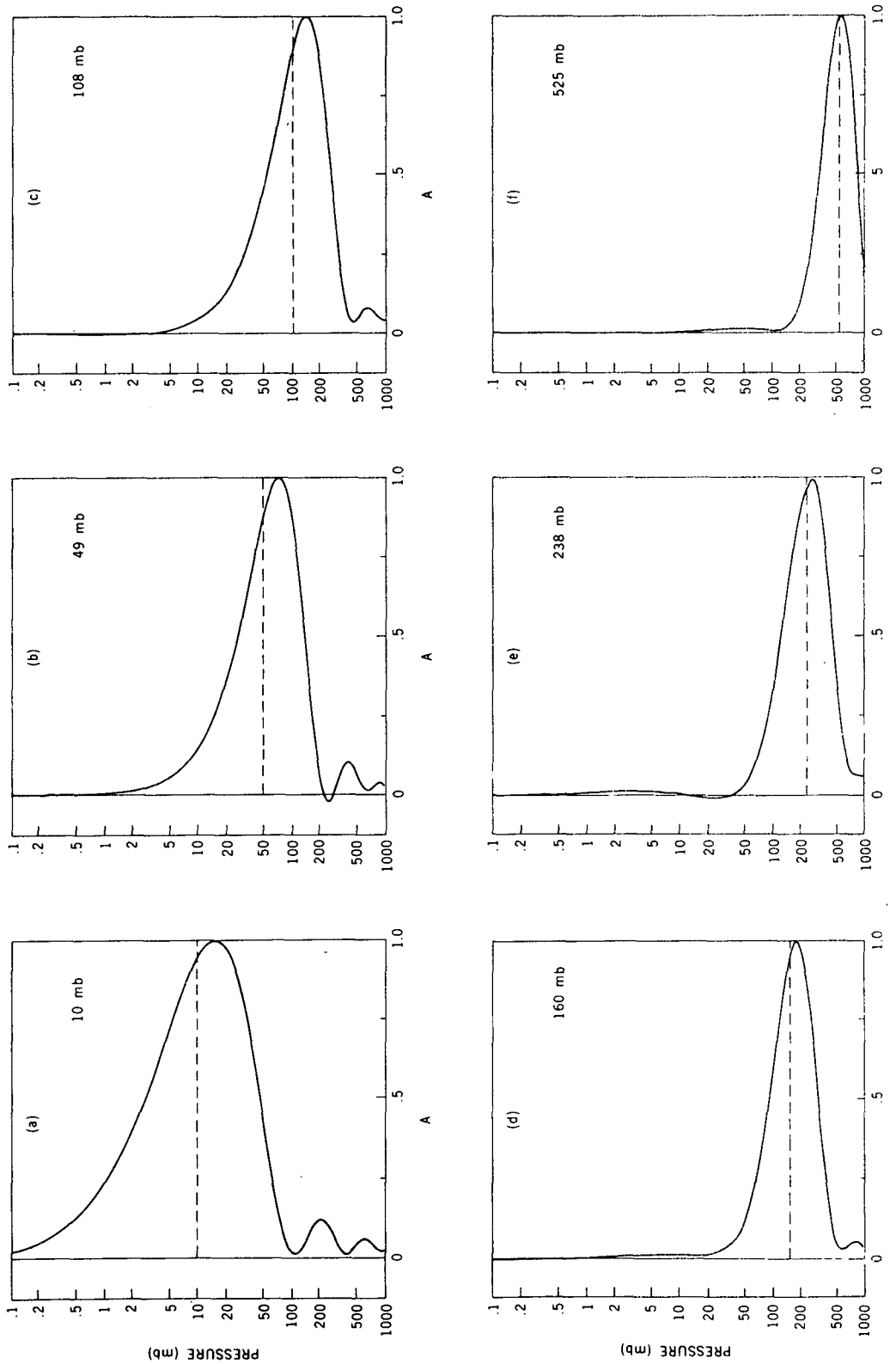

Figure 4. Averaging kernels for selected atmospheric levels. The level to which each kernel pertains is indicated by both a label and a broken line.

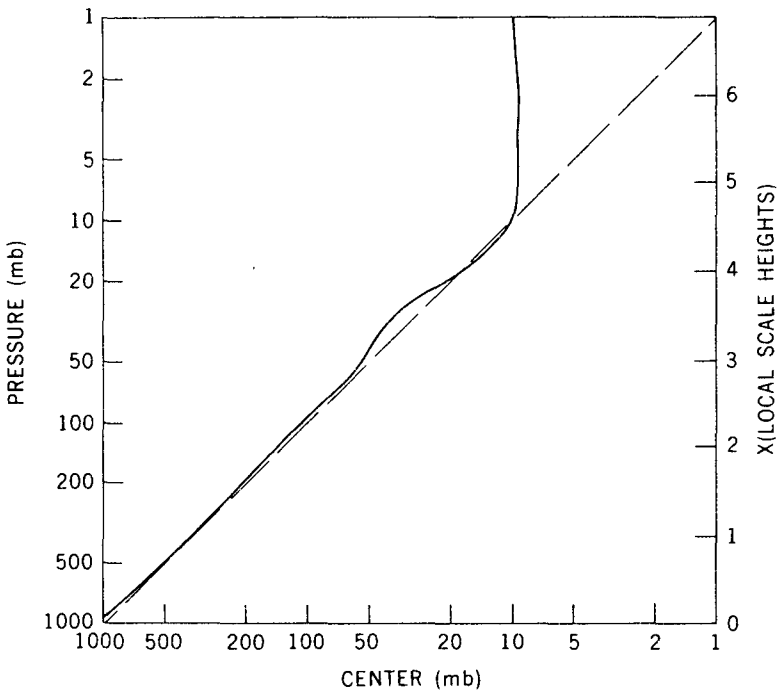

Figure 5. The averaging kernel center plotted as a function of atmospheric pressure level (solid curve). If the center of the kernel exactly coincided with the level to which the kernel pertained, the broken line would result.

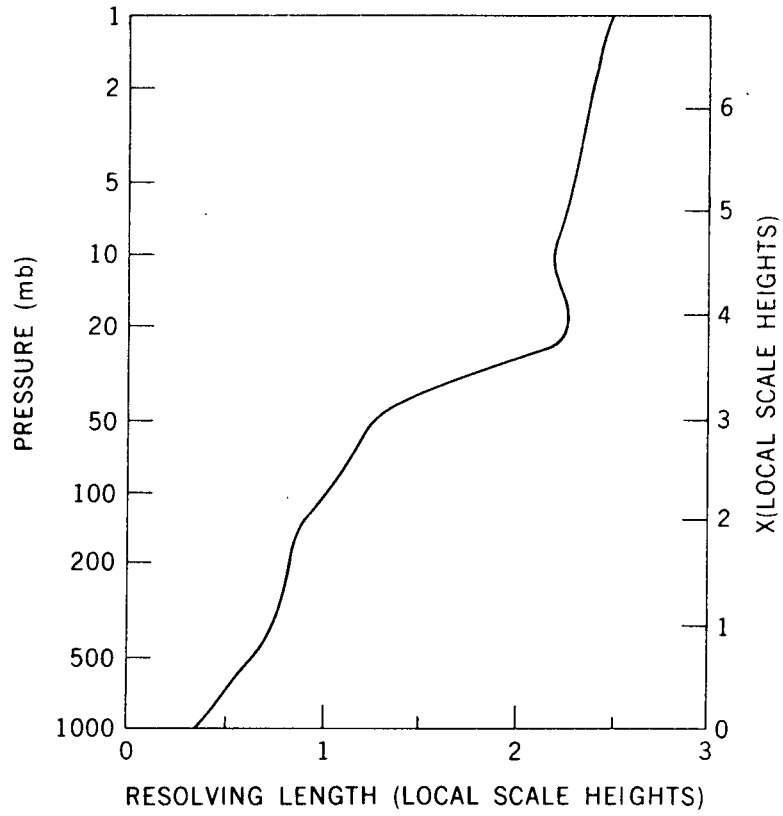

Figure 6. The resolving length plotted as a function of atmospheric level. The resolving length provides a measure of vertical resolution.